

Incorporation of Graphene oxide into Chitosan-Poly(acrylic acid) porous polymer nanocomposite for enhanced lead adsorption

Ruji P. Medina,^{a,b} Enrico T. Nadres,^a Florencio C. Ballesteros, Jr.^b and Debora F. Rodrigues^{a,*}

^aDepartment of Civil and Environmental Engineering, University of Houston, Houston, TX 77204-5003, USA

^bEnvironmental Engineering Graduate Program, College of Engineering, University of the Philippines, Diliman, Quezon City, 1101 Philippines

*Corresponding author: Tel.: +1 (713) 7431495; Email: dfrigirodurigues@uh.edu

SUPPLEMENTARY DATA

I. Characterization of Graphene Oxide

The preparation of the GO has been outlined in our other publication¹. The characterization of GO that has been used in this experiment is presented here.

A. FTIR (Fourier transform infrared) Spectroscopy

Oxygen-containing functional groups are shown in the FTIR bands of GO, indicating the successful preparation of the nanomaterial.¹ Peaks at 1061 and 1378 show the C-O-C stretching vibration and C-OH stretching, respectively. Peak at 1618 shows C=C stretching associated with the sp² character of the carbon skeletal network. The peak at 1718 represents the C=O stretching vibration of the -COOH functional group and peak at 3362 shows the -OH stretching vibration.

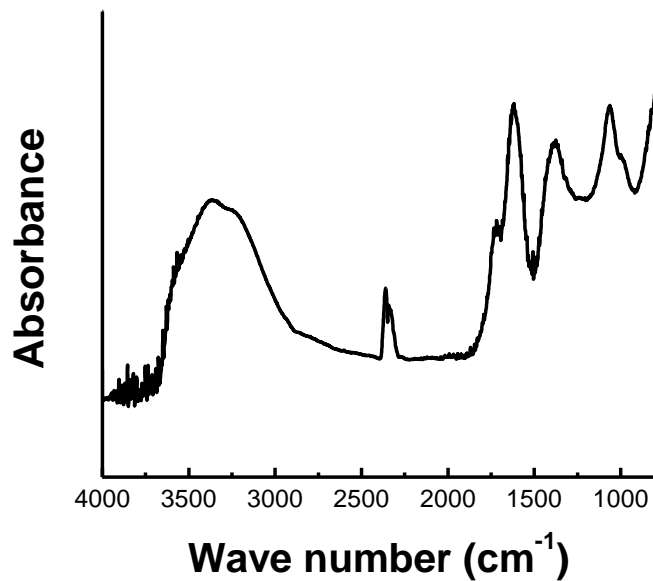
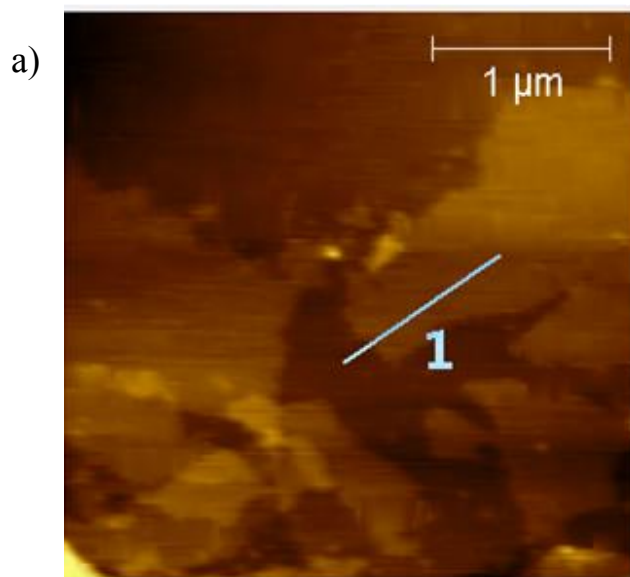


Fig. S1. FTIR spectra of graphene oxide.

B. AFM (Atomic Force Microscopy)

AFM analysis was done after spin coating of GO on silicon substrate (**Figure S2**).

Topography image of GO revealed that the height of GO is around 1 nm^2 .



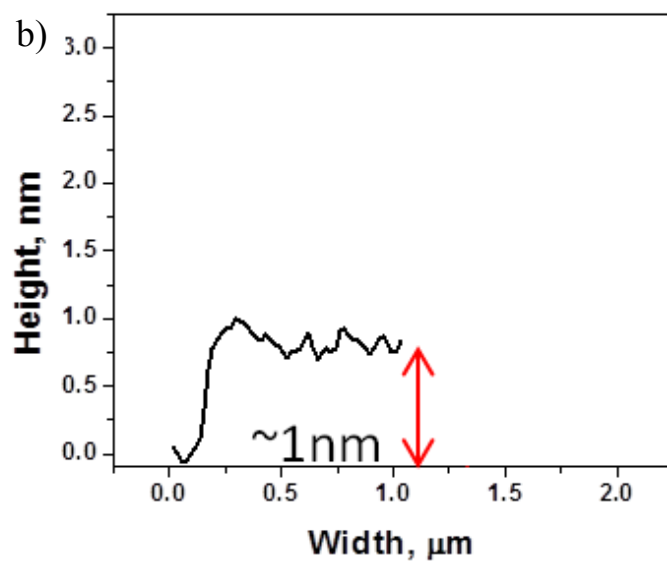


Figure S2. AFM analysis of GO a) topography image, b) height profile

C. XRD (X-Ray Powder Diffraction)

The GO nanosheet (**Figure S3**) exhibited a diffraction band at $2\theta = 11.1^\circ$. The computed d spacing is around 0.8 nm. The broad diffraction peak signifies that the sheets are in poor stacking condition, which suggests that the sample is single to few layers GO³.

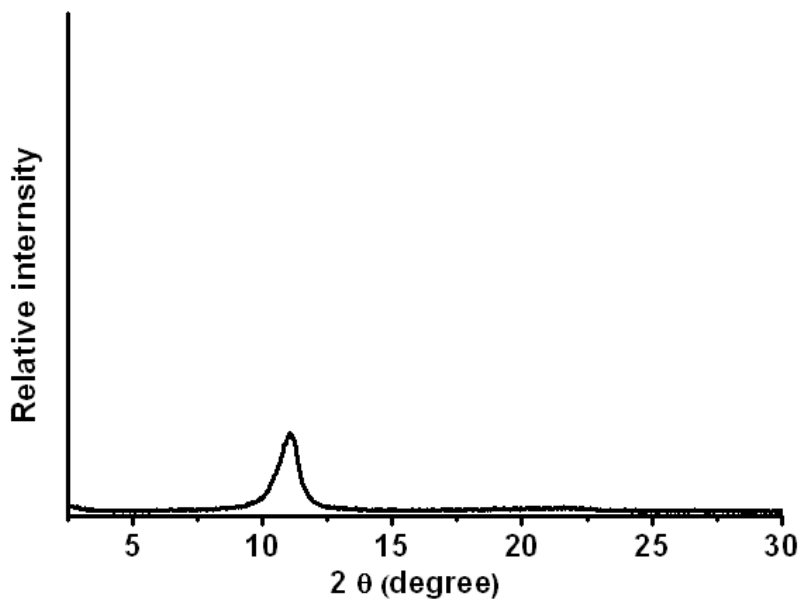


Figure S3. XRD Pattern of graphene oxide

D. XPS (X-ray Photoelectron Spectroscopy)

XPS analysis (**Figure S4a**) showed the functional groups present in the prepared GO ⁴. High resolution C 1s of GO showed an intense peak at 284.2 eV which corresponds to C-C bonds. Additional peak at 286 eV can be fitted into four peaks with different binding energies: 284.7 eV, 285.5 eV, 286.5 eV, and 288.9 eV assigned as C-C, C-OH, C-O-C, and C=O, respectively (**Figure S4b**) ⁵

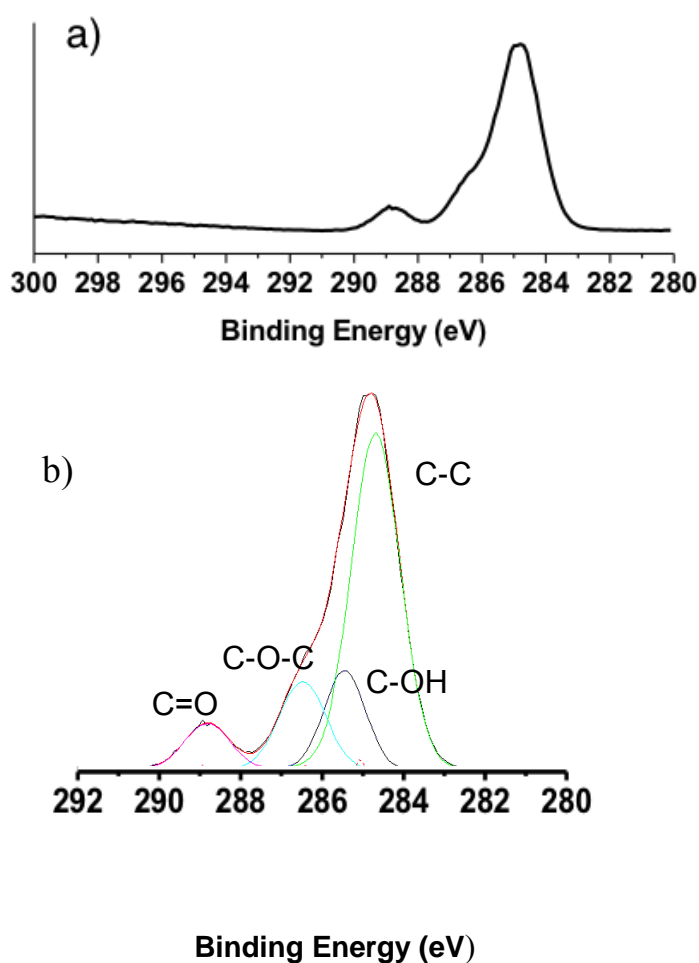


Figure S4. XPS Analysis of the prepared GO a) High resolution scan, b) Deconvoluted C1s peak.

2. Preparation of the polymer beads

Polymer composite solutions prepared as shown in **Figure S5**. Three types of beads were prepared for this study (**Table S1**). The bead CS-PAA contains only chitosan and PAA; while beads GO1 and GO5 has different concentration of GO. The water content of the hydrogel beads were determined. The differences in the water of hydration across the samples is due to the added GO.

The beads size range from 3–3.5 mm (**Figure S2**). CS-PAA has a light almost transparent color (Fig. S2, Panel A, left bead). Crosslinking using GLA resulted in yellow to brownish beads (Fig. S2, Panel A, right bead). Addition of GO has imparted a dark coloration onto the beads GO 1 and GO5 (Figure S2, Panels B and C, respectively). The prepared CS-PAA, GO1 and GO5 solutions showed good stability with no observable phase separation even after several months. The stability was maintained until hydrogel formation and enhanced by crosslinking using GLA.

Table S1. Chitosan beads prepared for this study

Beads	Composition			Water of hydration (%)
	Chitosan (%)	PAA (%)	GO (%)	
CS-PAA	2	1.5	0	97.95
GO1	2	1.5	1	97.85
GO5	2	1.5	5	97.74



Fig. S5. CS-PAA, GO1, and GO5 polymer solutions.



Figure S6. Chitosan hydrogel beads prepared in this study. (A) CS-PAA, (B) GO1 and (C) GO5 hydrogel beads have an average diameter of 3 mm.

3. Kinetic Experiments

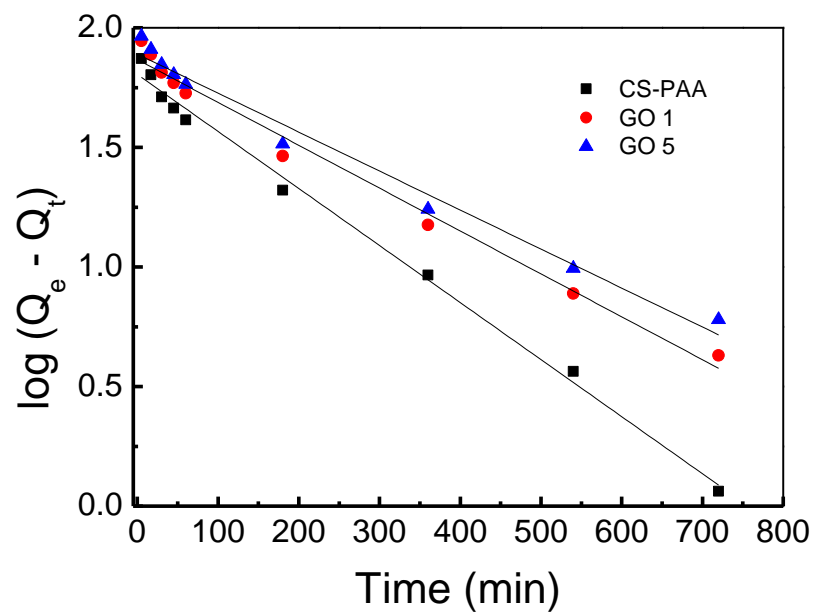


Fig. S7. Linearized plot for pseudo first-order kinetic model.

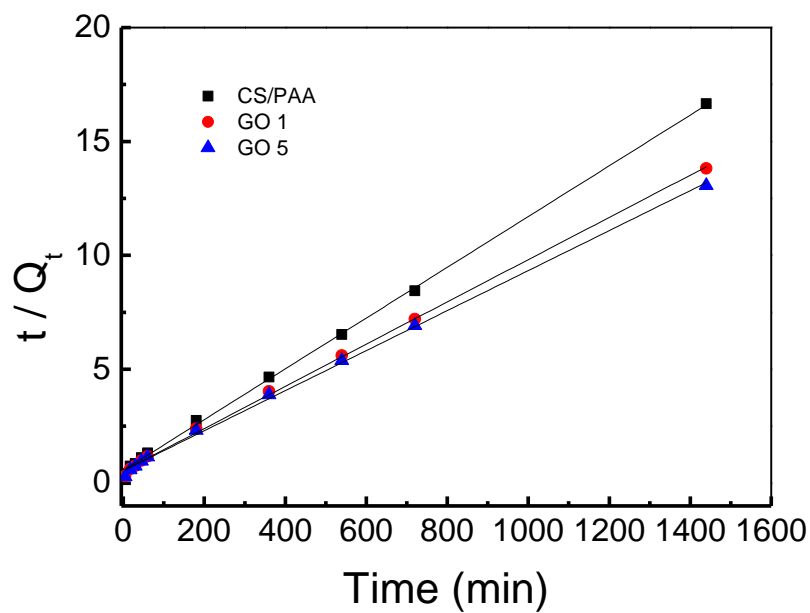


Fig. S8. Linearized plot for pseudo second-order kinetic model.

4. Energy-dispersive X-ray spectroscopy

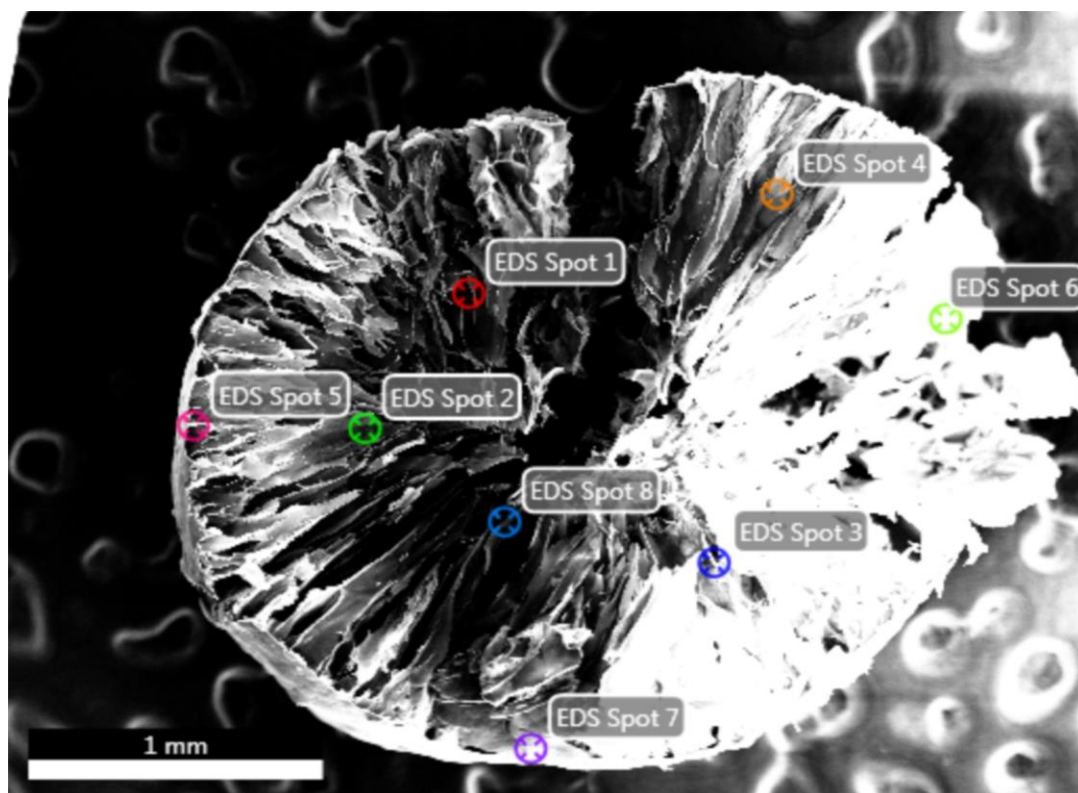


Fig. S4. Spots used in the EDS elemental analysis of the cross-section CS-PAA-GO beads.

Table S2. Elemental composition of random regions on the cross section of the CS-PAA-GO beads

Spot	% Weight							
	C	% Error	O	% Error	Au	% Error	Pb	% Error
1	57.82	6.71	39.01	12.63	--	--	3.17	49.00
2	45.6	7.94	28.42	11.19	20.27	8.76	0.38	67.13
3	50.72	7.06	28.89	10.85	15.79	8.24	0.26	67.47
4	47.1	7.62	29.53	11.00	17.98	8.98	0.19	71.26
5	55.13	6.65	39.56	11.99	--	--	5.3	18.9
6	46.83	6.99	35.62	10.00	13.36	8.67	0.34	63.38
7	52.20	11.27	23.54	22.55	--	--	24.25	19.36
8	42.2	9.99	25.80	11.12	26.35	7.46	0.59	63.12

5. References

1. Musico YLF, Santos CM, Dalida MLP, Rodrigues DF. 2014. Surface Modification of Membrane Filters Using Graphene and Graphene Oxide-Based Nanomaterials for Bacterial Inactivation and Removal. *ACS Sustainable Chemistry & Engineering* 2:1559-65
2. Mejias Carpio IE, Mangadlao JD, Nguyen HN, Advincula RC, Rodrigues DF. 2014. Graphene oxide functionalized with ethylenediamine triacetic acid for heavy metal adsorption and anti-microbial applications. *Carbon* 77:289-301
3. Chang BYS, Huang NM, An'amt MN, Marlinda AR, Norazriena Y, et al. 2012. Facile hydrothermal preparation of titanium dioxide decorated reduced graphene oxide nanocomposite. *International Journal of Nanomedicine* 7:3379-87
4. Ahmed F, Rodrigues DF. 2013. Investigation of acute effects of graphene oxide on wastewater microbial community: A case study. *Journal of Hazardous Materials* 256–257:33-9
5. Dreyer DR, Park S, Bielawski CW, Ruoff RS. 2010. The chemistry of graphene oxide. *Chemical Society Reviews* 39:228-40